

Pessimistic asynchronous sampling in high-cost Bayesian optimization

Amanda A. Volk¹, Kristofer G. Reyes², Jeffrey G. Ethier³, Luke A. Baldwin³

¹ *Air Force Science and Technology Fellow, Air Force Research Laboratory, Wright-Patterson Air Force Base, OH, 45433, United States*

² *Department of Materials Design and Innovation, University at Buffalo, Buffalo, NY 14260*

³ *Materials and Manufacturing Directorate, Air Force Research Laboratory, Wright-Patterson Air Force Base, OH 45433, United States*

Abstract

Asynchronous Bayesian optimization is a recently implemented technique that allows for parallel operation of experimental systems and disjointed workflows. Contrasting with serial Bayesian optimization which individually selects experiments one at a time after conducting a measurement for each experiment, asynchronous policies sequentially assign multiple experiments before measurements can be taken and evaluate new measurements continuously as they are made available. This technique allows for faster data generation and therefore faster optimization of an experimental space. This work extends the capabilities of asynchronous optimization methods beyond prior studies by evaluating four additional policies that incorporate pessimistic predictions in the training data set. Combined with a conventional greedy policy, the five total policies were evaluated in a simulated environment and benchmarked with serial sampling. Under some conditions and parameter space dimensionalities, the pessimistic asynchronous policy reached optimum experimental conditions in significantly fewer experiments than equivalent serial policies and proved to be less susceptible to convergence onto local optima at higher dimensions. Without accounting for the faster sampling rate, the pessimistic asynchronous algorithm presented in this work could result in more efficient algorithm driven optimization of high-cost experimental spaces. Accounting for sampling rate, the presented asynchronous algorithm could allow for faster optimization in experimental spaces where multiple experiments can be run before results are collected.

Introduction

Asynchronous Bayesian optimization algorithms enable greater flexibility in algorithm assisted experimental workflows. In most traditional scientific experimental procedures, experiments are conducted over distinct process steps. For example, in reaction chemistry research, a reaction process is often conducted in one experimental apparatus and the synthesized material is characterized with a separate analysis tool. For any single experiment, some portion of the equipment is available for use before the completion of the procedure, which means that an algorithm would have the opportunity to select additional tests to run before it has data from the prior experiment available to it. This issue

is further compounded in experimental environments that rely on a human within the experiment conduction and selection loop.

One strategy for resolving an incomplete utilization of resources is batch, also referred to as parallel, sampling. In batch sampling, a set of experiments are defined and conducted with complete utilization of experimental resources during each stage of an experimental process, then the measurements from that set of experiments are simultaneously returned to the algorithm for selection of the next set of experiments. This approach is suitable for select experimental environments, such as combinatorial screening platforms or high time cost measurements. However, batch sampling poses

several intuitive issues in sampling efficiency. First, while equipment utilization is improved, there is typically still equipment down time when alternating between the different stages of the experiments. Second, batch sampling often does not maximize data availability in algorithm decision making. Unless a batch sampling configuration is the optimal workflow for data generation throughput, there is typically a missed opportunity to complete an experiment and measurement that informs the experiment selection algorithm before conducting all the experiments in the set. Finally, batch methods are not suitable for experimental systems with time dependent outcomes. For example, if an experiment were to produce a material that degrades over time, batch methods would not result in a uniform time step between experiment and measurement, resulting in imprecise data generation.

In response to the constraints of batch sampling strategies, asynchronous sampling methods have recently been implemented in high-cost experimental environments.^[1] Shown in Figure 1, asynchronous sampling methods implement similar strategies to batch sampling by selecting multiple experiments without completing measurements, except in asynchronous designs, experiments are continuously measured and added to the data set while other experimental steps are being conducted. In an asynchronous Bayesian optimization design, there is a moving window buffer that contains placeholder data for the currently running experiments. This buffer set is appended to the real value data set for model training. When an experiment measurement completes, the real data replaces the placeholder data. Then, a new

experiment is selected, and the placeholder data is added to the buffer. Several strategies have been implemented to generate placeholder values in asynchronous Bayesian optimization, including local penalty strategies^[2-5] and greedy constant liar predictions^[1] among others.^[6,7] In prior studies, asynchronous sampling resulted in faster data generation rates and therefore faster approach to optimal experimental conditions.

In this work we present four alternative asynchronous sampling policies: (1) pessimistic constant liar, (2) descending pessimism constant liar, (3) ascending pessimism constant liar, and (4) lower confidence bounds liar. We benchmark these four policies with serial sampling and greedy constant liar asynchronous sampling on a selection of representative surrogate ground truth functions. The simulated optimization campaigns on surrogate functions showed that with an upper confidence bounds decision policy and a Gaussian Process regressor, the greedy constant liar policy and all three alternative policies outperformed serial sampling considerably when accounting for the improved sampling rate. Furthermore, we found that all three pessimism driven policies consistently performed competitively with serial sampling and in some cases significantly outperformed serial sampling when accounting for the number of experiments conducted. The three proposed strategies not only generate data at a faster rate than serial sampling, but they also select experiments equally or more efficiently. Implementation of the proposed algorithm has notable implications in asynchronous experiment conduction loops for high-cost experiments, and it could potentially improve the sampling efficiency of serial closed-loop systems.

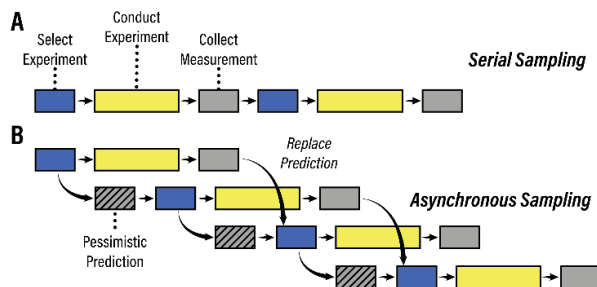


Figure 1. Illustration of asynchronous policy selection process versus serial selection.

Methods

Decision Policy

The asynchronous Bayesian optimization simulations were conducted using a modified BOBnd framework.^[8] In all simulations, the model was a scikit-learn^[9] Gaussian Process regressor with

a radial basis function kernel and a limited-memory BFGS optimizer, and the acquisition function was an upper confidence bounds policy as defined below:

$$X_{Next} = \operatorname{argmin}(y'(X) + \lambda\sigma(X)), \quad \lambda = \frac{5}{\sqrt{2}}$$

$$X = \langle x_1, x_2, \dots, x_D \rangle$$

where X_{Next} is the next set of experimental conditions, y' and σ are the model response mean prediction and standard deviation respectively as a function of the experimental conditions vector X , x_i is the condition input value for dimension i , D is the total number of dimensions in the input space, and λ is the exploration constant.

Asynchronous Predictions

The asynchronous sampling policy generates a vector of predicted values, referred to as the buffer array (B), for all incomplete experiments. For the simulations conducted in this work, the length of the buffer array (N_{Buffer}) varied between one to ten predicted samples, corresponding to one to ten simultaneously running experiments. Each of the five buffer policies – greedy, pessimistic, ascending pessimism, descending pessimism, and lower confidence bounds – fill in the buffer arrays – B_{Greed} , B_{Pess} , $B_{AscPess}$, $B_{DesPess}$, and B_{LCB} respectively – with the following equations:

$$B_{Greed} = \langle y'(X_{C+1}), y'(X_{C+2}), \dots, y'(X_{C+N_{Buffer}}) \rangle$$

$$B_{Pess} = \langle 0, 0, \dots, 0 \rangle$$

$$B_{AscPess} = \left\langle \frac{N_{Buffer} - 1}{N_{Buffer}} y'(X_{C+1}), \frac{N_{Buffer} - 2}{N_{Buffer}} y'(X_{C+2}), \dots, \frac{N_{Buffer} - N_{Buffer}}{N_{Buffer}} y'(X_{C+N_{Buffer}}) \right\rangle$$

$$B_{DecPess} = \left\langle \frac{0}{N_{Buffer}} y'(X_{C+1}), \frac{1}{N_{Buffer}} y'(X_{C+2}), \dots, \frac{N_{Buffer}}{N_{Buffer}} y'(X_{C+N_{Buffer}}) \right\rangle$$

$$B_{LCB} = \left\langle \operatorname{argmin}(y'(X_{C+1}) - \lambda\sigma(X_{C+1})), \operatorname{argmin}(y'(X_{C+2}) - \lambda\sigma(X_{C+2})), \dots, \operatorname{argmin}(y'(X_{C+N_{Buffer}}) - \lambda\sigma(X_{C+N_{Buffer}})) \right\rangle$$

where X_{C+j} is the input vector for the buffer position (j) after the most recent completed experiment (C). A pessimistic value is defined as the lower bound of the expected response range, which in the case of the *TriPeak* surrogate is zero. The pessimistic assumption, also referred to as censorship in prior works,^[10] has been leveraged in delay distribution contexts, but it has not been evaluated under uniform delay asynchronous sampling.

Surrogate Ground Truth

The surrogate ground truth function, $f(X)$, referred to as *TriPeak*, is an N -dimensional, triple Gaussian peak integrand function adapted from the BOBnd library,^[8] Surjanovic and Bingham,^[11] and Genz,^[12] and is defined with the equation below:

$$f(X) = c \left(b_1 \exp\left(\sum_{i=1}^D a_1^2 (x_i - \mu_1)^2\right) + b_2 \exp\left(\sum_{i=1}^D a_2^2 (x_i - \mu_2)^2\right) + b_3 \exp\left(\sum_{i=1}^D a_3^2 (x_i - \mu_3)^2\right) \right)$$

$$c = \frac{1}{D(b_1 + b_2 + b_3)}$$

$$a_1 = 4, \quad \mu_1 = 0.2, \quad b_1 = 0.3$$

$$a_2 = 1.5, \quad \mu_2 = 0.5, \quad b_2 = 0.2$$

$$a_3 = 4, \quad \mu_3 = 0.8, \quad b_3 = 0.6$$

where c is the normalization scalar, a_j is the peak width modifier, μ_j is the peak location, and b_j is the

peak height modifier for a single dimension of peak j . In the noisy simulations, the ground truth surrogate was sampled and added to the noise feature, which is attained by sampling from a normal probability distribution with a mean of zero and standard deviation specified by the set noise value – 0.01, 0.02, and 0.05 for 1%, 2% and 5% noise respectively.

Results

The four asynchronous sampling policies were studied with a five-dimensional *TriPeak* surrogate ground truth function, with the results shown in Figure 2. All five policies demonstrated some viability in accelerating optimization rates through parallel experimentation. However, the greedy policy exhibited significant losses in sampling efficiency when increasing the buffer length to four samples or higher. Additionally, no asynchronous

buffer length with a greedy policy outperformed serial sampling when evaluated as a function of the number of experiments. Among the four tested policies, a pure pessimistic policy had the highest and most consistent performance across all campaign replicates and buffer lengths, and the descending pessimism performed similarly. While the ascending pessimism policy performed more favorably than the greedy policy across all buffer lengths, the highest buffer length showed some indication of a less consistent or slower convergence onto the optimum.

For the pessimistic and descending pessimism policies, the median of campaign replicates reached optimal conditions more quickly than other tested methods for all buffer lengths; however, the four and nine buffer lengths more quickly reached a low inner quartile range of the best response across campaign replicates than equivalent one and two buffer lengths. All asynchronous policies leveraging

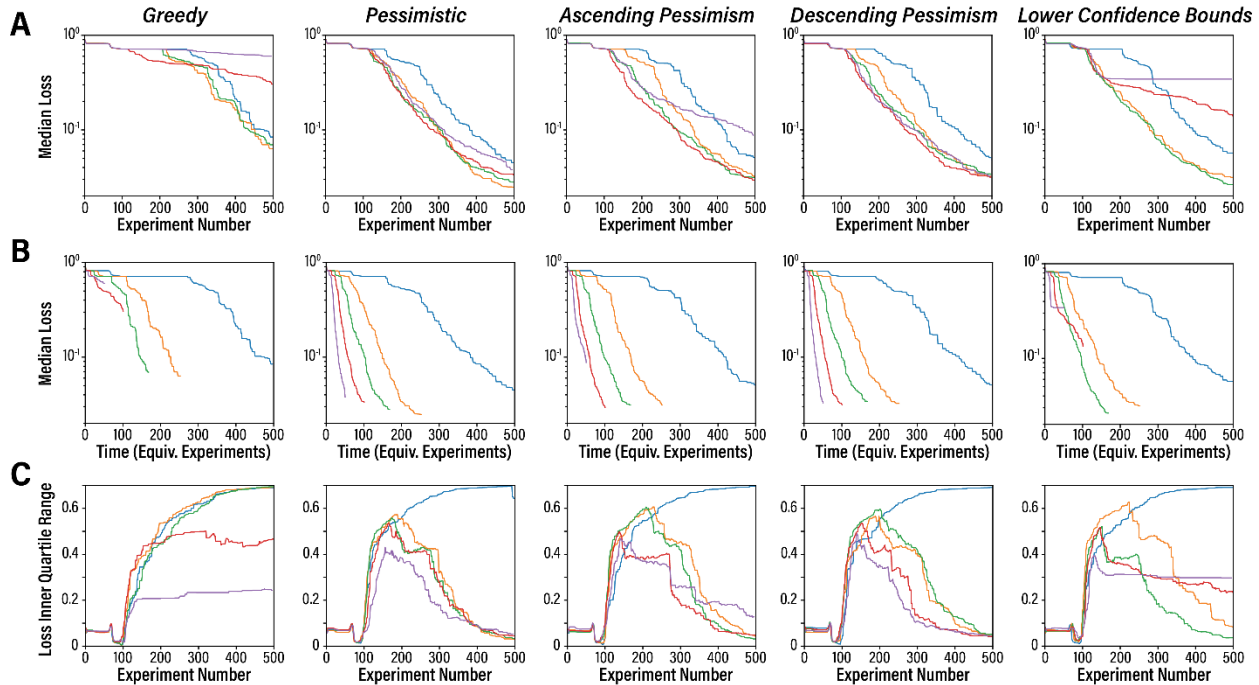


Figure 2. Simulation results of four asynchronous decision policies on five-dimensional *TriPeak*. The median loss across all 200 randomized simulated campaigns as a function of (A) the number of experiments and (B) the effective optimization time relative to a single experiment and (C) the inner quartile range of the loss as a function of experiment number across the four decision policies, (first column) greedy, (second column) pessimistic, (third column) ascending pessimism, (fourth column) descending pessimism, and (fifth column) lower confidence bounds. The no buffer replicates were repeated for each of the four policies.

pessimism indicated a reduction in the inner quartile range within five hundred experiments, while all serial and pure greedy policies continued to increase or plateau. These findings suggest that the presence of pessimism in asynchronous policies produces more effective and consistent optimization, and increasing the range of those pessimistic predictions can further increase the consistency with which campaigns reach optimal conditions. Additionally, the greatest algorithm improvement is observed after the inclusion of a single pessimistic prediction, i.e. one buffer length for the pessimistic, ascending pessimism, and descending pessimism policies. Significant improvements are observed with modest additions of pessimistic predictions, while greedy predictions either have no impact or decrease algorithm performance.

The lower confidence bounds policy performed equivalently to the pessimistic policy when evaluated over one and two buffer lengths; however, the policy appears to converge prematurely and perform worse than the serial policy at high buffer

lengths. Small buffer lower confidence bounds policies likely behave similarly to pessimistic policies in that the uncertainty near local optima is high enough to provide a sufficiently pessimistic hallucination. The failure at higher buffer lengths could be attributed to excessively confident models near local optima where clusters of buffer experiments are selected. In this latter case, the policy likely behaves more similarly to the greedy policy and provides insufficient pessimism to encourage exploration.

This pessimistic asynchronous method also demonstrates higher performance relative to serial sampling at higher dimensionalities. Shown in Figure 3, the serial policy outperforms all asynchronous pessimistic policy as a function of experiment number for two, three, and four-dimensional surrogate spaces. However, the asynchronous policies considerably outperformed the serial method for five and six dimensional spaces. It should also be noted that the asynchronous method provided a performance

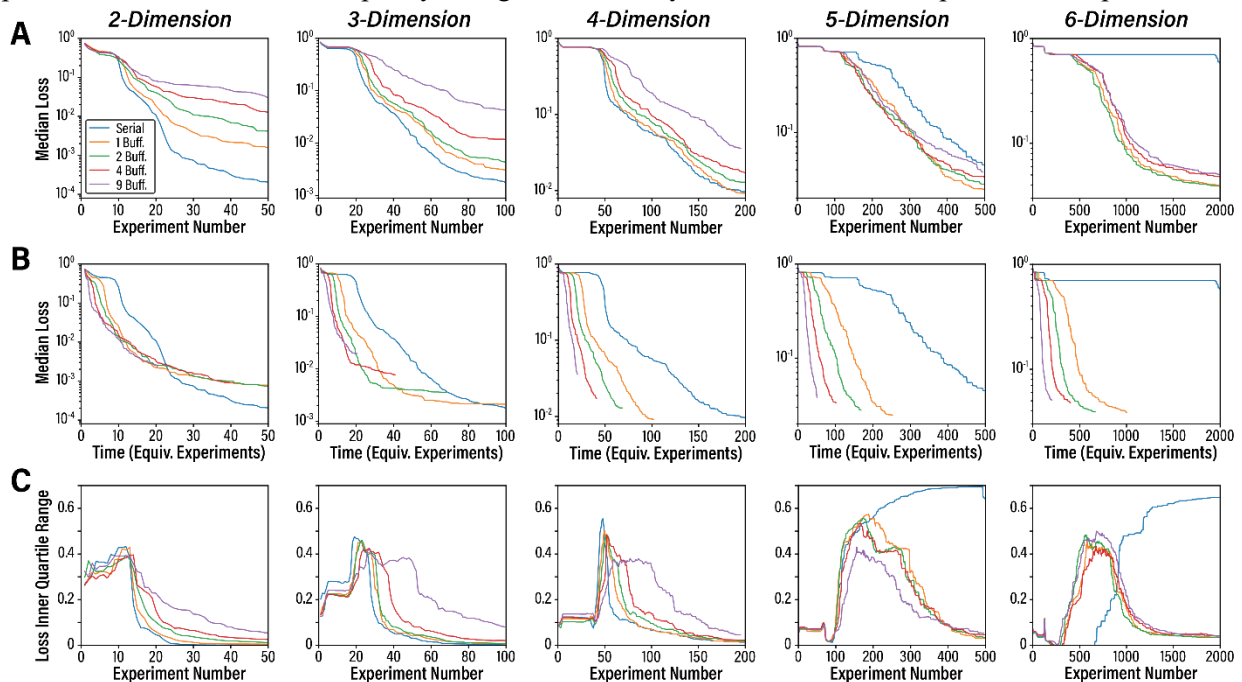


Figure 3. Simulation results of pessimistic decision policies on *TriPeak* at different dimensionalities and buffer lengths. The median loss across all randomized simulated campaigns as a function of (A) the number of experiments and (B) the effective optimization time relative to a single experiment and (C) the inner quartile range of the loss as a function of experiment number across (columns) two, three, four, five, and six-dimensional surrogate spaces. Each dimensional plot is the result of 200 replicates.

advantage for all five studied dimensions when considered as a function of experimentation time.

One potential explanation for the efficacy of pessimism assisted asynchronous sampling strategies is that the pessimistic predictions reduce the occurrence of premature convergence in upper confidence bounds policies. By forcing a pessimistic prediction on what the current model indicates is the optimal condition prevents resampling at that point, and in cases where replicates already exist outside the buffer, it increases model uncertainty at that point to enable improved exploration within the peak. This advantage becomes more dominant when the number of local minima – i.e. the dimensionality of the *TriPeak* function – increases.

The integration of the pessimistic prediction within the model training data set contrasts with prior pessimistic prediction methods on constant buffer length systems which implement a penalty region

over a defined area around the prior data point. It is possible that these penalty region methods could suffer from the curse of dimensionality as the volume covered by the defined penalty areas represents a smaller fraction of the overall parameter space.^[13]

A final study was conducted by introducing noise on the five-dimensional *TriPeak* surrogate ground truth function using the Pessimistic buffer policy across two to six dimensions. Shown in Figure 4, increasing the noise of the surrogate system resulted in less efficient optimization algorithms in most cases, but the serial policy at higher dimensions gained a performance advantage likely due to the normalization effect of noisy sampling. Like the no noise simulations, the serial policy outperformed the asynchronous policies for all noise levels at lower dimensionality, and the magnitude of the sampling penalty increased as the buffer size increased. Additionally, the introduction of noise negates any advantage with respect to experiment

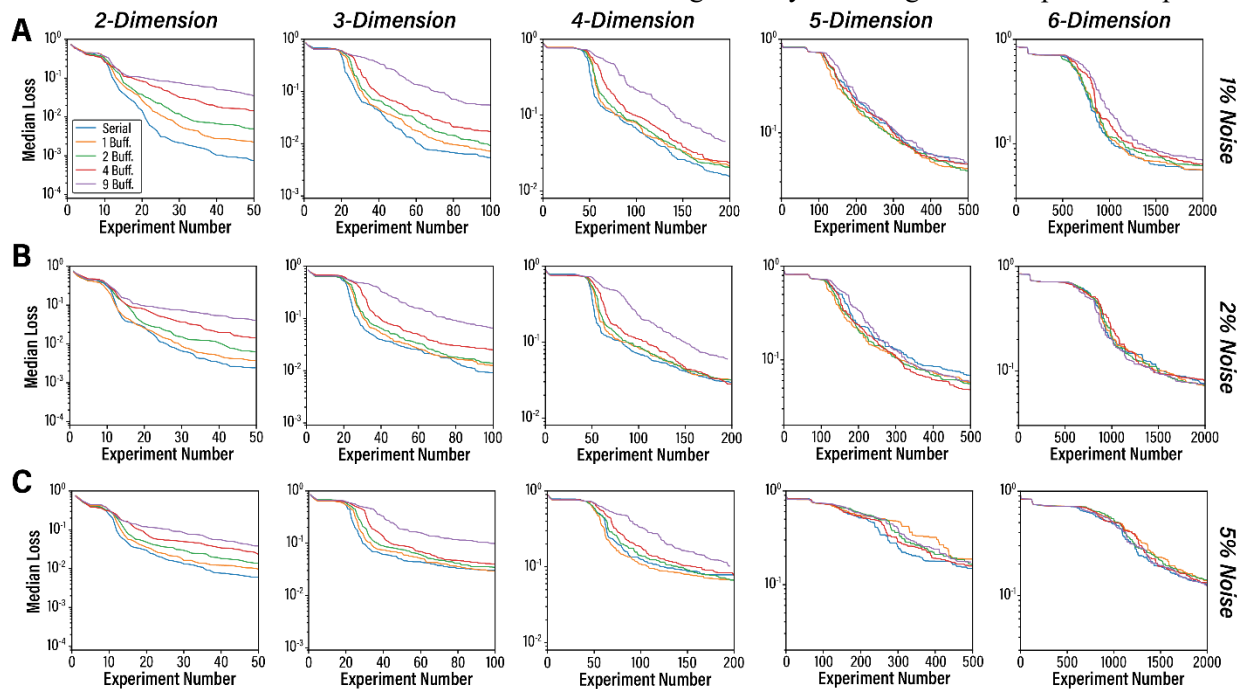


Figure 4. Simulation results of pessimistic decision policies on *TriPeak* at different dimensionalities and noise levels. The median loss across all randomized simulated campaigns as a function of (A) the number of experiments and (B) the effective optimization time relative to a single experiment and (C) the inner quartile range of the loss as a function of experiment number across (columns) two, three, four, five, and six-dimensional surrogate spaces. Each dimensional plot is the result of 200 replicates. The loss is calculated from the noiseless ground truth and does not reflect the values sampled from the surrogate during each trials campaign.

number attained by the buffer policies at five and six dimensions; however, the asynchronous policies substantially overlap with the results of the serial policy with respect to experiment number at these higher dimensions. This result further supports the notion that large buffers in pessimistic asynchronous sampling algorithms can provide faster optimizations with no or negligible impact on experimental efficiency.

By implementing pessimistic predictions through model integration, the asynchronous sampling policies presented here could more effectively navigate higher dimension parameter spaces through more efficient and comprehensive integration of pessimism. In the complex experimental spaces relevant to algorithm driven experimentation, asynchronous policies provide a notable advantage to serial algorithms when parallel operation is viable. Furthermore, pessimistic asynchronous policies may provide an additional advantage over greedy based hallucinations.

Conclusions

The asynchronous sampling policies presented in this work provide a valuable advancement over existing Bayesian optimization strategies for high-cost experimentation in serial experimental systems. Further implementation and development of the methods presented here, and other model-integrated pessimism, could result in more efficient algorithm driven experimentation and more effective parallelization of experimental processes.

References

- [1] F. Strieth-Kalthoff, H. Hao, V. Rathore, J. Derasp, T. Gaudin, N. H. Angello, M. Seifrid, E. Trushina, M. Guy, J. Liu, X. Tang, M. Mamada, W. Wang, T. Tsagaantsooj, C. Lavigne, R. Pollice, T. C. Wu, K. Hotta, L. Bodo, S. Li, M. Haddadnia, A. Wolos, R. Roszak, C.-T. Ser, C. Bozal-Ginesta, R. J. Hickman, J. Vestfrid, A. Aguilar-Granda, E. L. Klimareva, R. C. Sigerson, W. Hou, D. Gahler, S. Lach, A. Warzybok, O. Borodin, S. Rohrbach, B. Sanchez-Lengeling, C. Adachi, B. A. Grzybowski, L. Cronin, J. E. Hein, M. D. Burke, A. Aspuru-Guzik, *Science* **2024**, *384*, eadk9227.
- [2] J. Gonzalez, Z. Dai, P. Hennig, N. Lawrence, in *Proc. 19th Int. Conf. Artif. Intell. Stat.*, PMLR, **2016**, pp. 648–657.
- [3] A. S. Alvi, B. Ru, J.-P. Calliess, S. J. Roberts, M. A. Osborne, in *Proc. 36th Int. Conf. Mach. Learn.*, PMLR, **2019**, pp. 253–262.
- [4] J. P. Folch, R. M. Lee, B. Shafei, D. Walz, C. Tsay, M. Van Der Wilk, R. Misener, *Comput. Chem. Eng.* **2023**, *172*, 108194.
- [5] S. Takeno, H. Fukuoka, Y. Tsukada, T. Koyama, M. Shiga, I. Takeuchi, M. Karasuyama, in *Proc. 37th Int. Conf. Mach. Learn.*, PMLR, **2020**, pp. 9334–9345.
- [6] D. Eriksson, U. Ai, M. Pearce, J. R. Gardner, R. Turner, M. Poloczek, in *Proc. 33rd Int. Conf. Neural Inf. Process. Syst.*, **2019**, pp. 5496–5507.
- [7] J. Miguel Hernández-Lobato, J. Requeima, E. O. Pyzer-Knapp, A. Aspuru-Guzik, J. M. Hernández-Lobato, J. Requeima, E. O. Pyzer-Knapp, A. Aspuru-Guzik, in *Proc. 34th Int. Conf. Mach. Learn.*, PMLR, **2017**, pp. 1470–1479.
- [8] A. Volk, R. Epps, **n.d.**, DOI 10.5281/ZENODO.10644703.
- [9] F. Pedregosa, V. Michel, O. Grisel, M. Blondel, P. Prettenhofer, R. Weiss, J. Vanderplas, D. Cournapeau, F. Pedregosa, G. Varoquaux, A. Gramfort, B. Thirion, O. Grisel, V. Dubourg, A. Passos, M. Brucher, É. Duchesnay, *J. Mach. Learn. Res.* **2011**, *12*, 2825.
- [10] A. Verma, Z. Dai, B. Kian, H. Low, in *Proc. 39th Int. Conf. Mach. Learn.*, PMLR, **2022**, pp. 22145–22167.
- [11] S. Surfanovic, D. Bingham, “Virtual Library of Simulation Experiments: Test Functions and Datasets,” can be found

under
<https://www.sfu.ca/~ssurjano/about.html>,
2013.

- [12] A. Genz, in *Proc. Int. Conf. Tools, Methods Lang. Sci. Eng. Comput.*, Elsevier North-Holland, Inc, **1984**, pp. 81–94.
- [13] N. Altman, M. Krzywinski, *Nat. Methods* **2018**, *15*, 399.